Supplement of Biogeosciences, 23, 5185–5204, 2026
https://doi.org/10.5194/bg-23-5185-2026-supplement

Supplement of

Tracking centennial changes in algal community composition and biomass using subfossil pigments in a high mountain lake (Sierra Nevada, Spain)

Joana Llodrà-Llabrés et al.

Correspondence to: Carmen Pérez-Martínez (cperezm@ugr.es)

SUPPLEMENTARY FIGURES AND TABLES

Table S1. Location and environmental characteristics of the study lake in Sierra Nevada mountains. Range and mean values (in brackets) or single values of the chemical and biological parameters from water column measurements are shown. Range and mean values are from a minimum of four samples. TP, total phosphorus; TN, total nitrogen; Chl-a, chlorophyll-a.

	Borreguil Lake
Altitude (m asl)	2980
Lake area (ha)	0.18
Catchment area (ha)	50.9
Alpine meadows area (ha)	0.56
Maximum depth (m)	2.5
Maximum volume (m^3)	2070
Conductivity ($\mu S\ cm^{-1}$)	13-15 (14)
Alkalinity (meq L^{-1})	0.07-0.1 (0.09)
pH	6.3
Calcium (mg L^{-1})	0.8-1.1 (1.0)
Chl-*a* ($\mu g\ L^{-1}$)	1.4-1.7 (1.5)
TP ($\mu g\ L^{-1}$)	13-27 (18)
TN ($\mu g\ L^{-1}$)	180-380 (280)

Table S2. Pigments identified from lake sediments included in this study and their taxonomic affinities. The number of functional groups (FG) of the pigment molecular structure is also indicated for carotenoids.

Peak	RT (min)	PeakCode	Full name	lmax (nm)	Taxonomic affinity	FG
1	0.69	Ph_0	Chlorophyllide-a	432, 665	Chl-a degradation product, abundant in diatoms	
2	1.02	Ph_3	Chl-c1	441, 635	Diatoms and Chrysophytes	
3	1.04	Car_7_8	UVA2- Scytonemin	387	Cyanobacteria exposed to high UV radiation	4
4	1.09	Ph_5b	Chl-c2	448, 636	Cryptophyta, Dinoflagellates, Diatoms and Chrysophytes	
5	1.53	Car_5	Fucoxanthin	452	Chrysophytes and diatoms	5
6	1.44	Ph_2	Phaeophorbide-b1	438, 650	Chl-b degradation product (grazing processes)	
7	1.92	Ph_1a	Phaeophorbide-a	411, 664	Chl-a degradation product (grazing processes)	
8	2.19	Ph_2a	Phaeophorbide-b2	438, 650	Chl-b degradation product (grazing processes)	
9	2.32	Car_9z	Asthaxanthin	478	Zooplankton (Crustacea)	4
10	2.40	Car_17d'	Aphanizophyll	450, 477, 507	N2-fixing cyanobacteria	3
11	2.52	Car_10a	Diadinoxanthin	449, 479	Dinoflagellates, chrysophytes and diatoms	3
12	2.71	Car_12_5	Antheraxanthin	448, 477	Charophyceae, Rodophyta and vascular plants	3
13	2.91	Car_18	Alloxanthin	456, 484	Cryptophytes	2
14	3.11	Car_17	Diatoxanthin	456, 485	Diatoms and chrysophytes	2
15	3.21	Car_11	Lutein	448, 475	Chlorophyta	2
16	3.31	Car_12	Zeaxanthin	454, 483	Cyanobacteria, Chlorophytes	2
17	3.55	Car_16	Canthaxanthin	472	Cyanobacteria and zooplankton (Cladocera)	2
18	3.85	Ph_13	Chl-b	462, 650	Chlorophyta	
19	3.95	Car_17_3	Unknown	448, 475		
20	4.21	Ph_19a	allomer Chl-a	433, 663	Chl-a degradation product	
21	4.40	Ph_19	Chl-a	431, 662	Cyanobacteria, algae and vascular plants	
22	4.51	Ph_19e	epimer1 Chl-a	431, 662	Chl-a degradation product	
23	4.65	Ph_19e'	epimer2 Chl-a	431, 662	Chl-a degradation product	
24	4.73	Car_21	Echinenone	470	Cyanobacteria and zooplankton (Cladocera)	1
25	4.95	Ph_23	Phaeophythin-b1	435, 651	Chl-b degradation product (senescence)	
26	4.99	Car_25a	b-carotene	421, 454, 480	Cyanobacteria, algae and vascular plants	0
27	5.07	Ph_25	Phaeophythin-a1	410, 665	Chl-a degradation product (senescence)	
28	5.19	Ph_26	Phaeophythin-b2	436, 651	Chl-b degradation product (senescence)	
29	5.27	Ph_28	Phaeophythin-a2	410, 665	Chl-a degradation product (senescence)	

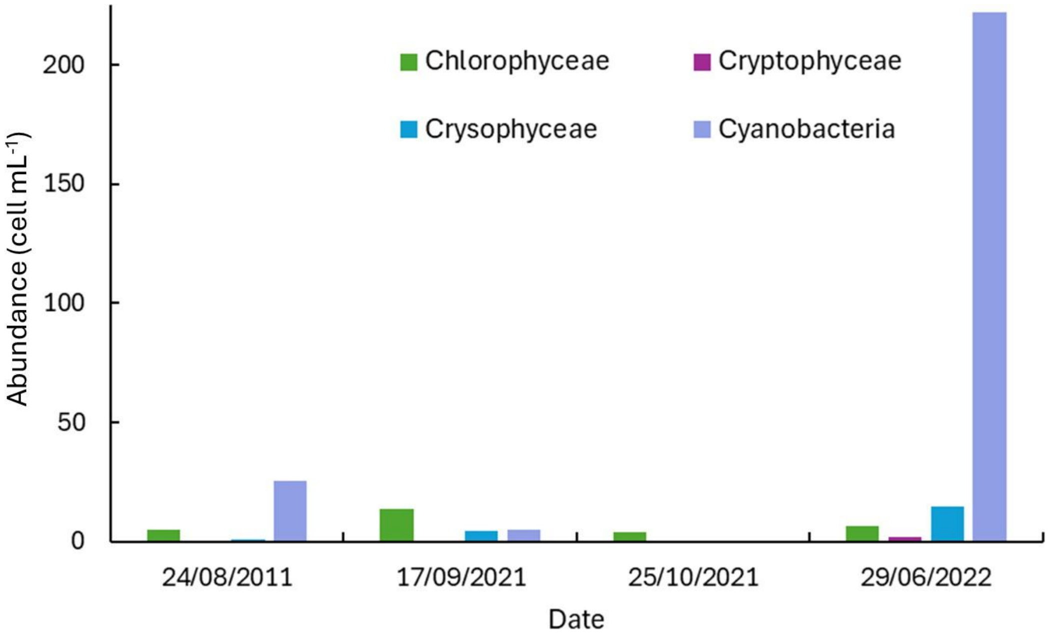

Figure S1. Planktonic algae composition and density in Borreguil Lake in selected dates of 2011, 2021 and 2022. 2022 was marked by a massive Saharan dust deposition event.

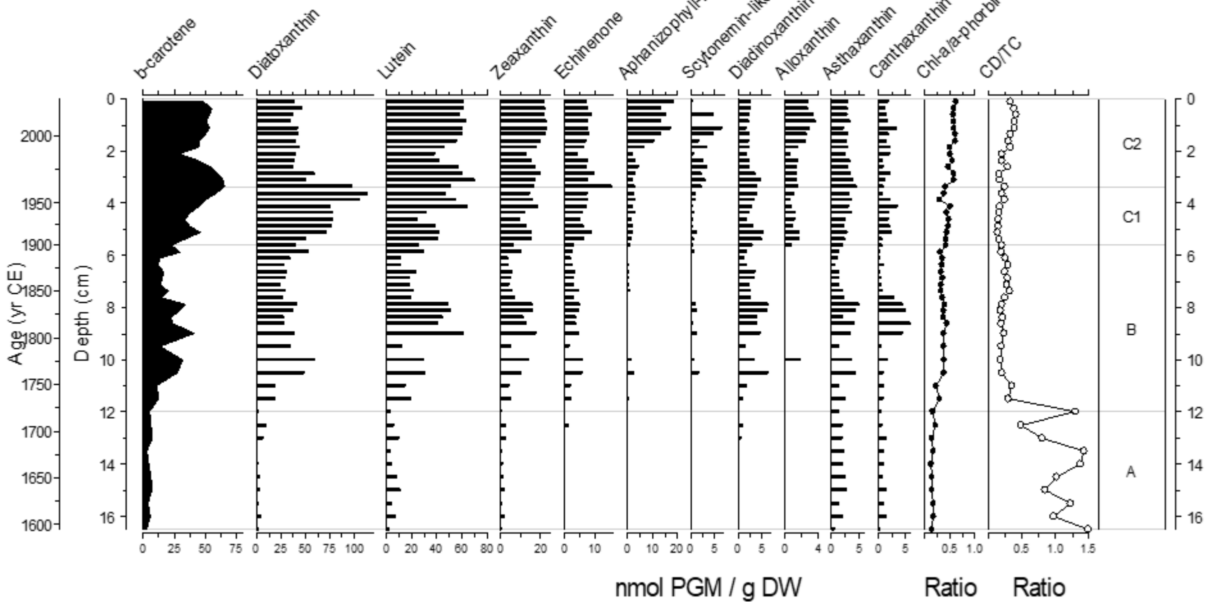

Figure S2. Pigment profiles of the 10 selected marker pigments and β-carotene expressed as concentrations (nmol PGM / g DW) and the ratios of Chl-a/a-phorbin as a Chla preservation index and the ratio CD/TC (chlorophyll-a derivatives vs. total carotenoids) as indicative of higher contribution of autochthonous production when the ratio is low. Four main biostratigraphic zones were established based on constrained incremental sum of squares partitioning of pigment concentration with Rioja-package version (0.9-15.2) (Juggins, 2017) using R version 3.5.3 (R Core Team 2019).

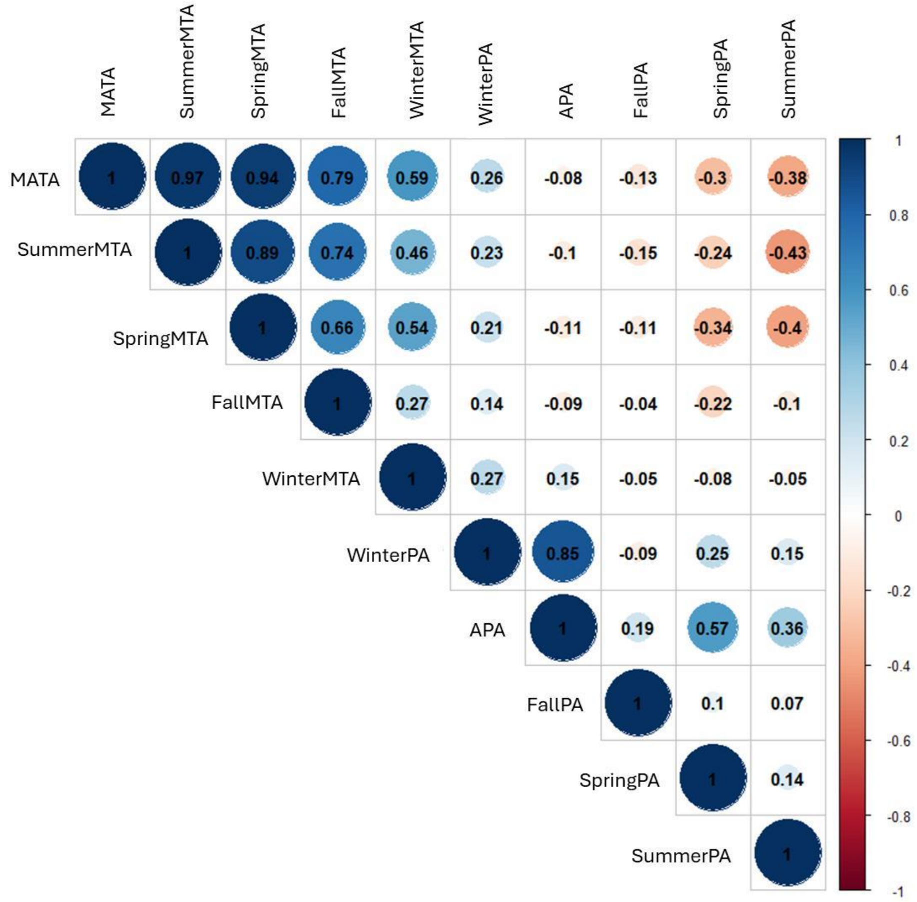

Figure S3. Pearson's correlation coefficient matrix between mean annual temperature anomaly (MATA), annual precipitation anomaly (APA), mean stational temperature anomalies (Summer-, Spring-, Fall- and Winter- MTA), and stational precipitation anomalies (Summer-, Spring-, Fall- and Winter- PA) for the period 1894-2020.

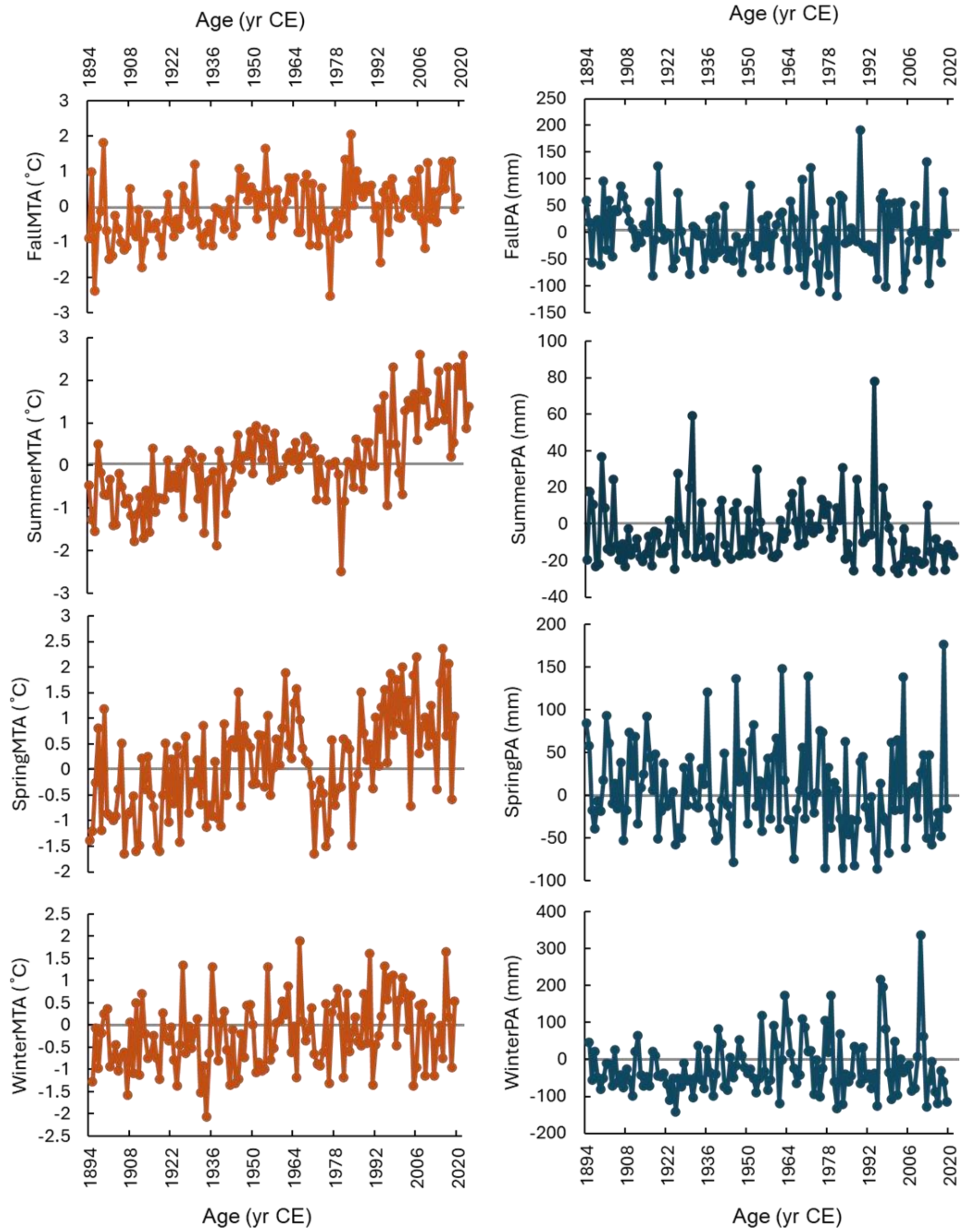

Figure S4. Mean stational temperature anomalies (Summer-, Spring, Fall- and Winter- MTA), and stational precipitation anomalies (Summer-, Spring-, Fall- and Winter- PA) for the period 1894-2020.